Thermal Imaging of Normal and Cranial Cruciate Ligament-Deficient Stifles in Dogs

Tomas Infernuso[1], DVM, Catherine A. Loughin[1], DVM, Diplomate ACVS & ACCT, Dominic J. Marino[1], DVM, Diplomate ACVS & ACCT, Cert CCRP, Scott E. Umbaugh[1], BSE, MSEE, PhD, and Patrick S. Solt[1], BSEE, MSCS

[1]Department of Surgery, Long Island Veterinary Specialists, Plainview, NY

Corresponding Author
Catherine A. Loughin, DVM, Diplomate ACVS & ACCT, Department of Surgery, Long Island Veterinary Specialists, 163 South Service Road, Plainview, NY 11803
E-mail: loughin1@yahoo.com

Submitted May 2009
Accepted November 2009

DOI:10.1111/j.1532-950X.2010.00677.x

Objective: To investigate the capability of thermography for differentiation between normal stifles and those with cranial cruciate ligament (CCL) rupture in dogs, initially with a full hair coat and 1 hour after clipping the hair coat.
Study Design: Prospective study.
Animals: Labrador Retrievers (n = 6) with normal stifle joints (controls) and adult dogs (n = 10) with CCL rupture.
Methods: Thermography was performed before, and 60 minutes after, clipping the hair coat from the pelvic limb. Stifle images were classified as normal or abnormal, then subclassified as clipped and unclipped hair coat. CCL deficiency was confirmed at surgery and thermographic images subsequently classified as abnormal before analysis with image processing software.
Results: Using image recognition analysis, differentiation between normal and CCL-deficient stifles in both clipped and unclipped dogs was 85% successful on cranial images, medial, caudal, and lateral images were between 75% and 85% successful. Although there were significant increases in skin temperature after clipping in both groups ($P < .0002$–$.0001$), there were no significant temperature differences between normal and CCL-deficient stifles when the entire stifle was examined.
Conclusion: Thermography was successful in differentiating naturally occurring CCL-deficient stifles in dogs, with a success rate of 75–85%. Clipping is not necessary for successful thermographic evaluation of the canine stifle.
Clinical Relevance: Thermography may be a useful imaging modality for diagnosis of CCL deficiency in dogs when CCL rupture is suspected but stifle laxity is not evident.

Stifle instability from cranial cruciate ligament (CCL) rupture is the most common cause of lameness in dogs.[1] The high incidence of CCL failure suggests premature ligament degeneration as an underlying cause. Predisposing factors include aging (especially large breed dogs), conformational abnormalities (straight pelvic limbs), immune-mediated disorders, genetic predisposition, excessive biomechanical stress, and decreased blood supply to the center of the ligament.[2–5]

Physical examination findings in dogs with CCL rupture can vary with chronicity. Dogs with acute CCL ruptures tend to have a none-to-partial weight-bearing lameness, with cranial drawer, tibial thrust, and joint effusion. Dogs with partial CCL ruptures may not be detectably lame, but may still have drawer, thrust, or effusion. Dogs with chronic CCL ruptures may have variable lameness, muscle atrophy, crepitus, cranial drawer, tibial thrust, medial buttress, and joint effusion. Tests demonstrating stifle laxity, such as the detection of cranial drawer and the tibial compression test, are diagnostic for CCL rupture; however, false-negative results secondary to periarticular fibrosis (medial buttress), and muscle contraction can affect test accuracy.[2] Synovial fluid analysis and cytologic evaluation can be used to detect inflammatory changes or presence of other causes of lameness (e.g., infectious and immune-mediated disease).[6]

Survey radiography of CCL-deficient stifles is routinely performed to assess the degree of periarticular osteophytes and to rule out other bony abnormalities; however its use in assessing intraarticular ligamentous structures is limited. Radiography with a translation device has recently been reported to enhance the detection of CCL rupture in dogs; however, its availability is limited.[7] Ultrasound diagnosis has been proven to be difficult because of lack of contrast between bone and soft tissue structures.[8] Computed tomography (CT) and CT

Veterinary Surgery 39 (2010) 410–417

arthrography are highly sensitive and specific for stifle pathology because of cross-sectional imaging and high resolution.[9] Magnetic resonance imaging (MRI) is the diagnostic modality of choice in human medicine for detection of anterior cruciate ligament rupture with $>95\%$ correlation with arthroscopy, and high specificity (92.2%) being reported.[10] Limitations of CT and MRI in dogs include high equipment cost, need for general anesthesia and the lack of universal availability. Arthroscopy or exploratory arthrotomy may be required when these tests are inconclusive. Diagnosis of CCL rupture can be challenging and failure to identify a lesion will likely affect the long-term clinical outcome of the patient. Additionally, the diagnosis of stifle instability secondary to CCL rupture can be confounded by concurrent disease of the ipsilateral coxofemoral joint.[11]

Thermal imaging is a valuable noninvasive imaging modality used for diagnosis of abnormal physiologic changes.[12–22] It is a diagnostic modality that records emission of surface heat from the skin and generates thermal patterns in the form of a color map. Warm regions, clinically associated with inflammation,[23] are related to an increase in local circulation and metabolic rate,[24] whereas cold regions are associated with decreased tissue perfusion secondary to a vascular shunt, infarction,[25] or changes in the autonomic nervous system.[23] Local dermal microcirculation, directly controlled by the sympathetic autonomic nervous system is responsible for the surface heat generated, not heat emanating from deeper tissues.[26] This explains the successful use of thermography in patients of all sizes regardless of the presence of excessive body fat.

Alterations in thermal pattern can be detected weeks before the onset of clinical signs or evidence of radiographic abnormalities.[23,27] Response to treatment, convalescent progress, and athletic training schedules can be monitored by serial use of thermography.[23] Thermography has high sensitivity but poor specificity and should be used in conjunction with other imaging modalities like ultrasound, radiography, CT, and MRI.[8,9,23,28–31]

Thermographic imaging systems have become increasingly sophisticated using focal plane array detectors with high-speed images and spatial resolution.[32] Image recognition software is being developed for objective analysis of thermal patterns.[33] In human medicine, thermographic imaging has been used for assessment of breast cancer,[33,34] vascular disorders,[35] burn patients,[33] scrotal varicocele,[36] pneumothorax,[37] radiculopathies,[38] intervertebral disk disease,[39] chiari malformation and syringomyelia,[40,41] pulpal blood flow of the teeth,[42] and joint disease.[43] For knee disorders in people, it has been used to detect sympathetic dysfunction in patellofemoral arthralgia,[44] chondromalacic patellae,[45] patellar tendonitis,[46] and rheumatoid arthritis.[47] Significant correlations have been found between clinical status and thermographic pattern changes for rheumatoid arthritis of the knee with regression of synovial thickening being confirmed on ultrasonography 3 months after treatment.[28] Good correlation has also been reported between changes in pain intensity and symmetry of thermal patterns for chronic knee pain (test efficiency 98%).[48]

Thermography use has been reported in equids, llamas, and cattle.[12–23,25,49–53] In cattle and llamas, use has been primarily in infectious and reproductive diseases,[12–21,53] whereas in equids, applications have been more diverse. For equine lameness detection, thermography used for disorders of tendons and ligaments, hoof (laminitis and navicular bone disease), joints, long bones, pelvic limb muscles, and the spine. [23,25,49–52] In acute tendonitis and suspensory desmitis, thermographic patterns appear has a focal increased area of heat in the normally elliptical isometric zone.[25] Laminitis can be detected thermographically because of temperature differences >1–$2^{\circ}C$ between the coronary band and hoof wall.[25] In horses with navicular disease, the thermal pattern is consistent, with a decreased area of heat associated with compromised blood flow.[25] Capsulitis and synovitis of most inflamed joints have a thermal pattern viewed from lateral to medial as an oval area of increased heat centered over the joint. Stress or fatigue fracture of the third metacarpal bone appears as hot spots on the medial or lateral aspect of the bone.[23] Gluteal and quadriceps myositis is associated with hot spots over the affected region.[49] In spinal disease causing back pain, the thermal pattern of the affected region appears as a cold spot because of altered sympathetic activity.[50]

In contrast to humans and horses, little is known about thermographic imaging of the canine stifle. Use of thermography in small animal medicine has been largely limited to research, with no clinical applications being reported.[54–59] Because of the noninvasive nature of this imaging modality without need for anesthesia or use of radiation in image generation, thermography may be a useful diagnostic screening technique for disorders of the canine stifle. Thus, our purpose was to compare thermal patterns and temperature gradients in the stifle region of clinically normal dogs, before and after hair clipping, with those of dogs with CCL-deficient stifles.

MATERIAL AND METHODS

Inclusion Criteria for CCL-Deficient Dogs

Within a 30-day period, all adult dogs with pelvic limb lameness were evaluated for further study. Inclusion criteria were dogs weighing >22.7 kg with unilateral CCL tear based on physical examination findings and confirmed by surgery. Dogs were excluded if there was evidence of metabolic, neurologic, or concurrent orthopedic disease.

Ten dogs (3 Labrador Retrievers, 3 mixed breed, and 1 each of Doberman, Golden Retriever and Akita; 1 intact and 1 neutered male and 1 intact and 7 spayed females), median weight 30.7 kg (range 26.1–45 kg) and median age 6.3 years (range 1–13 years) were selected for study. Preoperative complete blood count and serum biochemical profiles were considered normal. Two radiographic projections (craniocaudal, mediolateral) were obtained on each stifle.

Control Dogs

Six Labrador Retrievers (1 intact and 1 neutered male, 4 intact females) were selected from a training-breeding program (Guide Dog Foundation for the Blind, Smithtown, NY). Median age was 2.4 years (range 1–5 years) and median weight, 29.3 kg (range 27.3–34 kg). No abnormalities were detected by physical, laboratory, or radiographic examination.

Thermographic Imaging and Surgery

All dogs had limited exercise and were maintained in temperature-controlled runs and imaged at room temperature (20–24°C). A stand mounted infrared camera (Med 2000 IRIS, Meditherm Inc., Beaufort, NC) with a focal plane array amorphous silicone microbolometer was used. For real time data analysis the camera was connected to a laptop computer. To minimize thermal artifacts from manual contact, trained technicians handled dogs by the tail and head and latex gloves were worn at all times. To minimize background artifact, potentially created by temperature differences in exterior walls, the dogs were positioned in front of a uniform interior wall with the camera ~1 m from the dog. Thermographic imaging of cranial (AHL2), caudal (PHL2), medial (MHL2), and lateral (HLL2) views of the left (Fig 1) and right stifle (AHR2, PHR2, MHR2, and HRL2) were obtained. The region of the stifle was defined as the cranial aspect of the patella to the caudal aspect of the gastrocnemius muscle and the distal third of the femur to the proximal third of the tibia.

The 1st set of thermographic images was obtained with the hair coat intact. After the initial images were taken, the hair coat of the pelvic limb of interest was clipped using a #40 clipper blade in a surgical preparation fashion. Then the same imaging protocol was used for each dog 60 minutes after clipping, based on previous research findings.[54] Each image was coded with an "S" to denote those that were of clipped stifles (e.g., AHL2S).

A software program (Meditherm Inc.) was used to save, analyze, and review image data. Images were converted from black and white to a preset 8°C temperature scale and a 16-shade color map. We chose white and red to represent warmer temperatures and blue and black for cooler temperatures. The program calculated the mean, maximum, and minimum temperatures of each image. Image processing software (CVIPtools, Computer Vision and Image Processing Laboratory, Department of Electrical and Computer Engineering, School of Engineering, Southern Illinois University, Edwardsville, IL) was used for pattern recognition and to analyze and evaluate thermographic patterns.

After thermographic evaluation was complete, CCL-deficient dogs were anesthetized and in 5 stifles a fabellar-tibial suture was placed using monofilament nylon,[60,61] whereas in 4 dogs, a tibial plateau leveling osteotomy (TPLO) was performed using standard 3.5 mm TPLO plates.[3]

Statistical Analysis

Previously we found no differences between left and right sided measurements in dogs,[54] so we chose to analyze left stifles only in this study. If left stifle data were not available, data from the right stifle were used. Variables were compared between control (normal) stifles and those with confirmed CCL tear (abnormal stifles) at the 2 time points (full hair coat and 60 minutes after clipping). Mixed model repeated measures analysis of variance was used to compare the means of each of the variables across group and time. Results are reported as the adjusted mean ± SD.

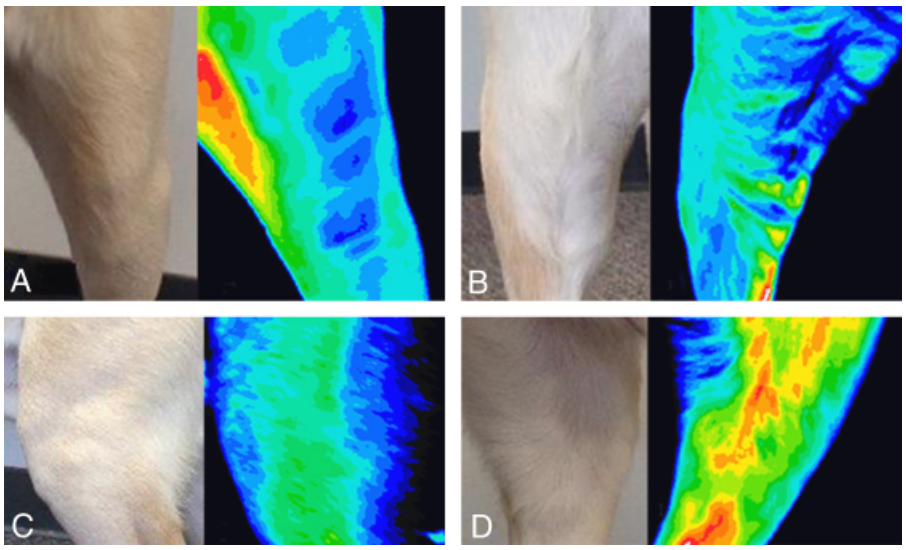

Figure 1 Thermal images. Photographs of the left stifle region and corresponding thermal images. (A) Cranial, (B) caudal, (C) lateral, and (D) medial views.

Imaging Pattern Analysis

An image processing software program that included a collection of computer vision and image processing routines was used to analyze images. Automated Computer Vision and Image processing-Algorithm Test and Analysis Tool (CVIP-ATAT) were created for the process of searching algorithms. CVIP-ATAT is composed of 3 layers: the top layer is the graphical user interface (GUI) which uses the C#.NET 2005, the middle communication (COM) layer which uses the C++.NET 2005, and the bottom layer is CVIPtools C Functions Libraries which uses C++.NET 2005. The GUI is in charge of the user's input, output, and displays analysis results. The COM layer is the connection between the GUI and CVIPtools C Functions Libraries. The CVIPtools C Functions Libraries consist of all image and data processing procedures and functions.

In experiments evaluating the stifle images the following variables were considered: Feature vector distance metric (Euclidean distance); features (5 texture features: energy, inertia, correlation, inverse difference, and entropy; 5 histogram features: mean, SD, skew, energy, and entropy); classes: normal clipped, abnormal clipped, normal unclipped. and abnormal unclipped; classification method: K-nearest neighbor, with K = 3; temperature color normalization: none; and data normalization: standard normal density (SND) and soft-max.

To simplify coding for image pattern analysis, the left pelvic limb codes were used. The 1st set of these experiments included the AHL2, AHL2S, HLL2, HLL2S, MHL2, MHL2S, PHL2, PHL2S images. Two primary sets of experiments were run: (1) normal versus abnormal unclipped, (2) normal versus abnormal clipped.

RESULTS

Statistical Analysis

There were significant interactions between group (normal versus abnormal) and time (full hair coat versus 60 minute after clipping); i.e., temporal changes did not depend on group. There were no significant differences between groups; however, for each variable there were significant increases in temperature after clipping (*P*-values range from $< .0002$ to $< .0001$; Table 1).

Table 1 Means and Standard Deviation

Group	Time	N	Variable	N	Mean	SD
Normal stifles	Full-coat	6	AHLMax	6	28.78	1.02
			AHLMin	6	24.08	1.06
			AHLAve	6	26.30	0.43
			HLLMax	6	28.48	0.81
			HLLMin	6	23.35	2.26
			HLLAve	6	26.77	0.71
			MHLMax	6	30.93	1.21
			MHLMin	6	25.97	1.19
			MHLAve	6	28.95	1.04
			PHLMax	6	27.88	1.24
			PHLMin	6	22.40	1.44
			PHLAve	6	24.53	1.12
	Postclipping (60 minutes)	6	AHLMax	6	32.13	0.91
			AHLMin	6	27.90	1.07
			AHLAve	6	30.07	0.85
			HLLMax	6	32.88	0.67
			HLLMin	6	28.65	0.74
			HLLAve	6	31.43	0.69
			MHLMax	6	33.68	0.90
			MHLMin	6	29.88	2.38
			MHLAve	6	32.38	1.05
			PHLMax	6	32.65	0.73
			PHLMin	6	28.40	1.14
			PHLAve	6	30.97	0.76
Abnormal	Full-coat	10	AHLMax	10	29.00	2.72
			AHLMin	10	24.59	2.43
			AHLAve	10	26.94	2.01
			HLLMax	10	29.12	1.88
			HLLMin	10	24.23	2.19
			HLLAve	10	27.19	2.14
			MHLMax	10	31.91	1.13
			MHLMin	10	25.95	2.23
			MHLAve	10	29.42	1.61
			PHLMax	10	29.25	2.82
			PHLMin	10	23.27	2.21
			PHLAve	10	25.51	3.12
	Postclipping (60 minutes)	10	AHLMax	10	32.61	1.34
			AHLMin	10	28.10	1.68
			AHLAve	10	31.15	1.42
			HLLMax	9	32.82	1.04
			HLLMin	9	28.91	1.24
			HLLAve	9	31.48	0.99
			MHLMax	10	33.57	1.50
			MHLMin	10	28.38	1.42
			MHLAve	10	31.85	1.62
			PHLMax	10	32.58	1.35
			PHLMin	10	27.82	1.39
			PHLAve	10	30.28	1.32

AHL, cranial stifle; HLL, lateral stifle; MHL, medial stifle; PHL, caudal stifle.

Imaging Pattern Analysis

Computer pattern analysis was able to differentiate CCL-deficient stifles from controls. In the cranial view of normal stifles there was a more uniform and cooler pattern, blue for the patella and blue to green in the parapatellar regions. The medial and lateral views were also uniform in pattern distribution, but the medial color pattern was warmer (blue to green for the lateral side and green to yellow for the medial). The caudal views also had a more uniform cooler pattern of blue. CCL-deficient stifles had the same blue pattern for the patella, but a warmer parapatellar region (yellow to orange to red) on the cranial views (Fig 2). Likewise, the medial, lateral, and caudal views had a pattern that was warmer in regions over bone (yellow to orange). Clipped images were similar in pattern to images of unclipped stifles, but the color scale was warmer.

There were 48,112 experiments performed. Cranial (AHL2) images provided the best results and consistency for classification of normal versus abnormal, and clipped and unclipped both achieved 85% success. The clipped images overall had more experiments with this success rate. Medial (MHL2) image results for the clipped were not as

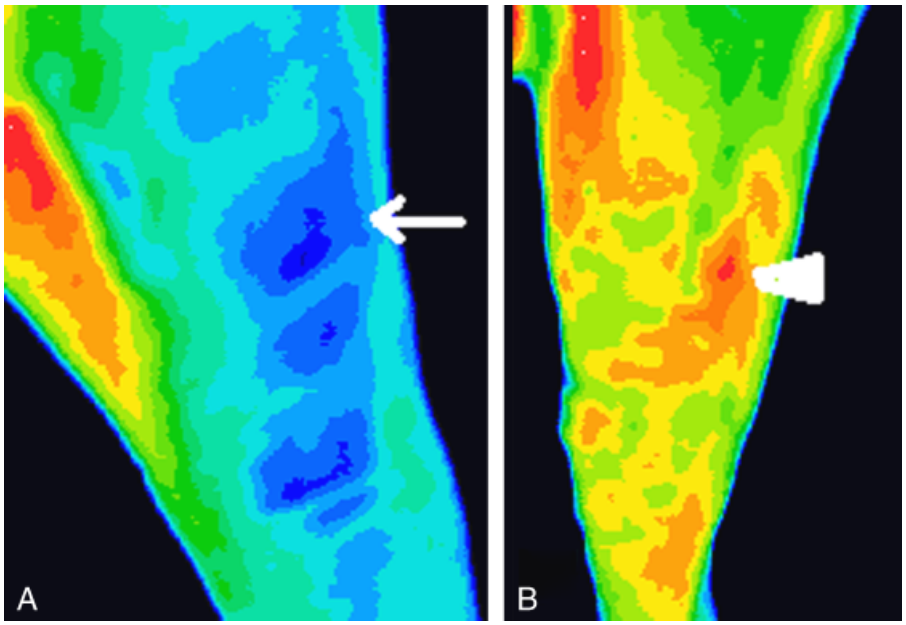

Figure 2 Normal cranial stifle thermal image (A), and cranial cruciate-deficient stifle (B) thermal image. Note the cooler region denotes the patella (white arrow), and the warmer region denotes the inflamed joint (white arrowhead).

accurate as the unclipped. Unclipped success rate was 85% and clipped 77%. Examination of the images reveals that the views are different, possibly because of difficulty in getting a thermograph image of the inside of the limb in a standing dog. Lateral (HLL2) image results were not as good with a maximum success rate of 75%. Clipped and unclipped gave equally consistent results. With the caudal (PHL2) images the clipped images achieved better results than the unclipped. The clipped had a maximum success of 85%, and unclipped 78%. SND versus soft-max data normalization revealed that they were equally successful. Texture distances of 5, 6, and 7 were also equally successful.

For the SND and the soft-max data normalizations a total of 3007 experiments for each image view were performed by varying the input feature set and the texture distance. All permutations of the 10 input features were used. The cranial image views (AHL2) had the most consistent and best results, with a maximum classification rate of 85% (Tables 2).

DISCUSSION

Computer pattern analysis was successful in differentiating CCL-deficient stifles from those with intact CCL. Cranial (AHL2) images provided the best results and consistency for classification of normal versus abnormal stifles. In human thermography, the anterior stifle image is the most useful for identification of diseases of the knee.[44] Osteoarthritic and rheumatoid knees have thermographic patterns consistent with regional elevated temperature (red and white spots) beside the patella on the anterior views. Conversely, thermal patterns of normal knees on the anterior view appear as uniform and blue (cold spot) because of the heat-shield effect of the patella.[44] The altered thermal pattern of patellar tendonitis has a discrete localized area of elevated temperature (red spot) directly overlying the region of the patellar tendon, disrupting the normal symmetrical thermal gradient from the center of the joint outward of normal knees.[46] Lastly, chondromalacic patellar thermal patterns consistently have various degrees of asymmetry secondary to the disappearance of the thermal gradient between the prepatellar zone, the coldest area (blue spot) and the popliteal fossa, the warmest (red spot) seen in normal knees.[45] We found these same pattern types on the cranial thermal images of dogs with CCL tears.

Medial (MHL2) image results for the stifles were not as accurate. Examination of the images revealed that the

Table 2 SND and Softmax Data Normalization

Image View	Clipped or Unclipped	SND Data Normalization: Max Classification Success Rate Normal Versus Abnormal	Softmax Data Normalization: Max Classification Success Rate Normal Versus Abnormal
AHL2	Unshaved	11/13 = 85%	11/13 = 85%
AHL2S	Shaved	11/13 = 85%	11/13 = 85%
HLL2	Unshaved	9/13 = 69%	9/13 = 69%
HLL2S	Shaved	9/12 = 75%	9/12 = 75%
MHL2	Unshaved	11/13 = 85%	11/13 = 85%
MHL2S	Shaved	10/13 = 77%	10/13 = 77%
PHL2	Unshaved	11/14 = 79%	10/14 = 71%
PHL2S	Shaved	11/13 = 85%	11/13 = 85%

AHL, cranial stifle; HLL, lateral stifle; MHL, medial stifle; PHL, caudal stifle; SND, standard normal density.

Veterinary Surgery 39 (2010) 410–417

positional views were slightly different, which may have affected computer analysis. This positional inconsistency was possibly because of the difficulty in having the dogs stay in position for this specific thermographic view. All images were obtained in a standing position. To accurately obtain the image without superimposition of the contralateral limb, the handler elevated the contralateral limb adjacent to the flank region and the camera was placed under the dog. These constraints may have been the cause of the inconsistency in success for this view.

Lateral (HLL2) image results were not as successful as the cranial, caudal, and medial views. Although regional temperature analysis found the medial side to be slightly warmer than the lateral sides in all dogs, this alone could not explain the diminished success of computer pattern analysis for the lateral view. Anatomic differences in the autonomic regulation of regional stifle cutaneous perfusion may explain the differences found in pattern analysis between the lateral and other views.

Statistically, no significant differences in regional temperatures between normal canine stifles and those with CCL ruptures were detected. We arbitrarily set the boundaries of the regions of interest using anatomic landmarks. Analyzing average temperatures of such large areas, relative to the likely small anatomic region of pathologic change, may have resulted in attenuation of significant temperature differences. Analyzing many smaller regions might have yielded areas of significant difference between regions.

Images of stifles with clipped hair coats had similar thermographic pattern to controls but the temperature scale was warmer. This phenomenon is consistent in multiple species (equids, llamas, dogs) and occurs because of the insulating properties of the hair coat. Readings after hair coat removal maybe elevated because they are representative of the actual skin temperature.[22,23,51–54] Our study design was based on a previous dog study that found normalization of skin temperature 1 hour after clipping.[54] It is unknown if the thermographic pattern and changes in the temperature scale found in dogs after clipping the hair coat would show continued cooling after 24 hours as reported in llamas.[53] The impact of the length and thickness of the hair coat on the thermographic pattern and temperature scale remains unknown.

Thermographic evaluation has been reported as a sensitive imaging modality that helps in early recognition of injuries and in establishing remedial therapy before other clinical methods of assessment. The lack of specificity and inability to identify causes, limit using thermography as the sole diagnostic modality. Therefore, thermography can play a role in screening dogs suspected of having CCL rupture, especially when the diagnosis is not apparent on physical examination. As advances in technology enhance the accuracy of thermal imaging equipment, increases in the scope of applications of thermal imaging have resulted in greater access to affordable cameras. Medical infrared imaging cameras remain more expensive than their industrial grade counterparts and manufactured with the specific needs of the medical practice in mind.

Limitations of this study were related to the small number of dogs evaluated, and the uniform hair coat length of the dogs studied. The impact of different types of hair coats warrants further investigation. The evaluation of the thermograms performed > 1 hour after hair coat clipping is necessary to assess the long-term impact of clipping on thermal patterns.

We concluded that thermography can be successfully used to differentiate CCL-deficient stifles from those with intact CCL. Clipping the hair coat was not necessary for successful evaluation. Owners reluctant to clip their dogs for diagnostic imaging may consider thermographic evaluation in dogs with pelvic limb lameness suspected of having a CCL tear. Future work should be done to evaluate the use of thermography as a screening tool for other stifle pathologies such as meniscal tears, osteochondrosis, caudal cruciate tears, patellar diseases, and collateral ligament damage.

REFERENCES

1. Hayashi K, Manley PA, Muir P: Cranial cruciate ligament pathophysiology in dogs with cruciate disease: a review. *J Am Anim Hosp Assoc* 2004;40:385–390
2. Moore KW, Read R: Rupture of the cranial cruciate ligament in dogs—part 1. *Compend Contin Educ Pract Vet* 1996;18: 223–233
3. Slocum B, Slocum TD: Tibial plateau leveling osteotomy for repair of cranial cruciate ligament rupture in canine. *Vet Clin North Am Small Anim Pract* 1993;23:777–795
4. Tirgari M: The surgical significance of the blood supply of the canine stifle joint. *J Small Anim Pract* 1978;19:451–462
5. Niebauer G, Wolf B, Bashe RI, et al: Antibodies to canine collagen type II and I in dogs with spontaneous cruciate ligament rupture and osteoarthritis. *Arthritis Rheum* 1987; 30:319–327
6. Barrett JG, Hao Z, Graf BK, et al: Inflammatory changes in ruptured canine cranial and human anterior cruciate ligaments. *Am J Vet Res* 2005;66:2073–2080.
7. Lopez MJ, Hagquist W, Jeffrey SL, et al: Instrumented measurement of in vivo anterior–posterior translation in the canine knee to assess anterior cruciate integrity. *J Orthop Res* 2004;22:949–954
8. Gnudi G, Bertoni G: Echographic examination of the stifle joint affected by cranial cruciate ligament rupture in the dog. *Vet Radiol Ultrasound* 2001;42:266–270
9. Samii VF, Dyce J: Computed tomographic arthrography of the normal canine stifle. *Vet Radiol Ultrasound* 2004;45: 402–406
10. Crawford R, Walley G, Bridgman S, et al: Magnetic resonance imaging versus arthroscopy in the diagnosis of knee pathology, concentration on meniscal lesions and ACL tears: a systematic review. *Br Med Bull* 2007;84:5–23
11. Powers MY, Martinez SA, Lincoln JD, et al: Prevalence of cranial cruciate ligament rupture in a population of dogs with lameness previously attributed to hip dysplasia: 369 cases. *J Am Vet Med Assoc* 2005;227:1109–1111

12. Heath AM, Pugh DG, Sartin EA, et al: Evaluation of the safety and efficacy of testicular biopsies in llamas. *Theriogenology* 2002;58:1125–1130
13. Purohit RC, Carson RL, Riddell MG, et al: Peripheral neurogenic thermogenic thermoregulation of the bovine scrotum. *Thermol Int* 2007;17:138–142
14. Tyler JW, Angle KL, Carson RL, et al: Bradycardia, altered thermographic patterns, and dysphonia associated with cervical laxity in a Ankole-Watusi bull. *Am J Vet Med Assoc* 1991;199:767–768
15. Spire MF, Drouillard JS, Galland JC, et al: Use of infrared thermography to detect inflammation caused by contaminated growth promotant ear implants in cattle. *J Am Vet Med Assoc* 1999;215:1320–1324
16. Heath AM, Carson RL, Purohit RC, et al: Effects of testicular biopsy in clinically normal bulls. *J Am Vet Med Assoc* 2002;220:507–512
17. Colak A, Polat B, Okumus Z, et al: Short communication: early detection of mastitis using infrared thermography in dairy cows. *J Dairy Sci* 2008;91:4244–4248
18. Rainwater-Lovett K, Pacheco JM, Packer C, et al: Detection of foot-and-mouth disease virus infected cattle using infrared thermography. *Vet J* 2009;180:317–324
19. Stewart M, Webster JR, Verkerk GA, et al: Non-invasive measurement of stress in dairy cows using infrared thermography. *Physiol Behav* 2007;92:520–525
20. Schaefer AL, Cook NJ, Church JS, et al: The use of infrared thermography as an early indicator of bovine respiratory disease complex in calves. *Res Vet Sci* 2007;83:376–384
21. Benington IC, Biagioni PA, Crossey PJ, et al: Temperature changes in bovine mandibular bone during implant site preparation: an assessment using infrared thermography. *J Dent* 1996;24:263–267
22. Purohit RC: Use of thermography in veterinary medicine, in Lee MHM, Cohen JM (eds): *Rehabilitation Medicine and Thermography*. Wilsonville, OR, Impress Publications, 2008, pp 129–141
23. Eddy AL, Van Hoogmoed LM, Snyder JR: The role of thermography in the management of equine lameness. *Vet J* 2001;162:172–181
24. Love TJ: Thermography as an indicator of blood perfusion. *Ann NY Acad Sci* 1980;335:429–437
25. Turner TA: Thermography as an aid to the clinical lameness evaluation. *Vet Clin N Am Equine Pract* 1991;7:311–338
26. Peter L: *Meditherm Manual of Clinical Thermology*. Beaufort, Meditherm Inc., 2004
27. Ben-Eliyanu DJ: Infrared thermographic imaging in the detection of sympathetic dysfunction in patients with patellofemoral pain syndrome. *J Manipulative Physiol Ther* 1992;15:164–170
28. Van Holsbeeck M, Van Holsbeeck K, Gevers G, et al: Staging and follow-up of rheumatoid arthritis of the knee. Comparison of sonography, thermography, and clinical assessment. *J Ultrasound Med* 1988;7:561–566
29. D'Anjou MA, Moreau M, Troncy E, et al: Osteophytosis, subchondral bone sclerosis, joint effusion and soft tissue thickening in canine experimental stifle osteoarthritis: comparison between 1.5 T magnetic resonance imaging and computed radiography. *Vet Surg* 2008;37:166–177
30. Seong Y, Eom K, Lee H, et al: Ultrasonographic evaluation of cranial cruciate ligament rupture via dynamic intra-articular saline injection. *Vet Radiol Ultrasound* 2005;46: 80–82
31. Vande Berg BC, Lecouvet FE, Poilvache P, et al: Anterior cruciate ligament tears and associated meniscal lesions: assessment at dual-detector spiral CT arthrography. *Radiology* 2002;223:403–409
32. Ring EF: The historical development of thermal imaging in medicine. *Rheumatology (Oxford)* 2004;43:800–802
33. Head JF, Elliott R: Infrared imaging: making progress in fulfilling it's medical promise. *IEEE Eng Med Biol Mag* 2002;21:80–85
34. Gautherie M, Haehnel P, Walter J, et al: Thermovascular changes associated with in situ and minimal breast cancers. *J Reprod Med* 1987;32:833–842
35. Verheye S, DeMeyer GR, Krams R, et al: Intravascular thermography: immediate functional and morphological vascular findings. *Eur Heart J* 2004;25:158–165
36. Tucker AT: Infrared thermographic assessment of the human scrotum. *Fertil Steril* 2000;74:802–803
37. Rich PB, Dulabon GR, Doullet CD, et al: Infrared thermography: a rapid, portable, and accurate technique to detect experimental pneumothorax. *J Surg Res* 2004;120: 163–170
38. So YT, Aminoff MJ, Olney RK: The role of thermography in the evaluation of lumbosacral radiculopathy. *Neurology* 1989;39:1154–1158
39. Doman I, Illes T: Thermal analysis of the human intervertebral disc. *J Biomech Biophys Methods* 2004;61: 207–214
40. Koyanagi I, Iwasaki Y, Isu T, et al: Thermographic findings of syringomyelia. *No Shinkeib Geka* 1988;16:1149–1154
41. Fujimoto A, Matsumura A, Nakamura K, et al: Chiari malformation type I associated with familial spastic paraplegia: report of a surgical treated case. *Child Nerv Syst* 2005;21:336–338
42. Kells BE, Kennedy JG, Biagioni PA, et al: Computerized infrared thermographic imaging and pulpal blood flow: part1. A protocol for thermal imaging of human teeth. *Int Endod J* 2000;33:442–447
43. Gratt BM, Sickles EA, Wexler CE: Thermographic characterization of osteoarthrosis of the temporomandibular joint. *J Orofac Pain* 1993;7:345–353
44. Devereaux MD, Parr GR, Lachmann SM, et al: Thermographic diagnosis in athletes with patellofemoral arthralgia. *J Bone Joint Surg Br* 1986;68:42–44
45. Vujcic M, Nedeljkovic R: Thermography in the detection and follow up of chondromalacia patellae. *Ann Rheum Dis* 1991; 50:921–925
46. Mangine RE, Siqueland KA, Noyes FR: The use of thermography 398 for the diagnosis and management of patellar tendinitis. *J Orthop Sports Phys Ther* 1987;9:132–140
47. Inoue K, Nishioloa J, Kobori T, et al: The use of thermography in the assessment of the rheumatoid knee—the

thermographic index and the heat distribution index. *Ryumachi* 1990;30:356–361

48. Sherman RA, Sherman CJ, Bruno GM: Thermographic correlates of chronic pain: analysis of 125 patients incorporating evaluations by a blind panal. *Arch Phys Med Rehabil* 1987;68:273–279
49. Turner T: Thermography as an aid in the localization of upper hind limb lameness. *Pferdeheilkunde* 1996;12:632–634
50. Graf von Schweinitz D: Thermographic diagnostics in equine back pain. *Vet Clin N Am Equine Pract* 1999;15:161–177
51. Turner TA, Fessler JF, Lamp M, et al: Thermographic evaluation of horses with podotrochliosos. *Am J Vet Res* 1983;44:535–539
52. Tunley BV, Henson FMD: Reliabilty and repeatability of thermographic examination and the normal thermographic image of the thoracolumbar region in the horse. *Equine Vet J* 2004;36:306–312
53. Heath AM, Navarre CB, Simpkins A, et al: A comparison of surface and rectal temperatures between sheared and non-sheared alpacas (*Lama pacos*). *Small Rumin Res* 2001;39:19–23
54. Loughin CA, Marino DJ: Evaluation of thermographic imaging of the limbs of healthy dogs. *Am J Vet Res* 2007; 68:1064–1069
55. Um SW, Kim Ms, Lim JH, et al: Thermographic evaluation for the efficacy of acupuncture on induced chronic arthritis in the dog. *J Vet Med Sci* 2005;67:1283–1284
56. Dobi I, Kekesi V, Toth M, et al: Endothelin-induced long-lasting mesenteric vasoconstriction: a hypothetical mechanism of non-occlusive intestinal infarction. *Acta Chir Hung* 1991;32:199–208
57. Adachi H, Becker LC, Ambrosio G, et al: Assessment of myocardial blood flow by real-time infrared imaging. *J Surg Res* 1987;43:94–102
58. Daniel W, Klein H, Hetzer R, et al: Thermocardiography—a method for continuous assessment of myocardial perfusion dynamics in the exposed animal and human heart. *Thorac Cardiovasc Surg* 1979;27:51–57
59. Stein LE, Pijanowski GJ, Johnson AL, et al: A comparison of steady state and transient thermography techniques using a healing tendon model. *Vet Surg* 1988;17:90–96
60. DeAngelis M, Lau RE: A lateral retinacular imbrication technique for the surgical correction of anterior cruciate ligament rupture in the dog. *J Am Vet Med Assoc* 1970; 157:79–84
61. Olmstead ML: The use of orthopedic wire as a lateral suture for stifle stabilization. *Vet Clin North Am Small Anim Pract* 1993;23:735–753